Int J Adv Manuf Technol (2014) 72:1527–1535
DOI 10.1007/s00170-014-5766-y

ORIGINAL ARTICLE

Chipping minimization in drilling ceramic materials with rotary ultrasonic machining

Jun Wei Liu · Dae Kyun Baek · Tae Jo Ko

Received: 11 March 2012 / Accepted: 6 March 2014 / Published online: 23 March 2014

Abstract Ultrasonic machining (USM) has been considered as a new cutting technology that does not rely on the conductance of the workpiece. USM presents no heating or electrochemical effects, with low surface damage and small residual stresses on workpiece material, such as glass, ceramics, and others; therefore, it is used to drill microholes in brittle materials. However, this process is very slow and tool wear dependent, so the entire process has low efficiency. Therefore, to increase microhole drilling productivity or hole quality, rotary ultrasonic machining (RUM) is considered as a strong alternative to USM. RUM, which presents ultrasonic axial vibration with tool rotation, is an effective solution for improving cutting speed, precision, tool wear, and other machining responses beyond those of the USM. This study aims to reduce the microchipping or cracking at the exit of the hole, which inevitably occurs when brittle materials are drilled, with consideration of tool wear. To this end, response surface analysis and desirability functions are used for experimental optimization. The experimental results showed that the proposed RUM scheme is suitable for microhole drilling.

Keywords Ultrasonic vibration · Rotary ultrasonic machining · Tool wear · Exit chipping · Response surface analysis · Optimization

J. W. Liu · T. J. Ko (✉)
School of Mechanical Engineering, Yeungnam University, 214-1, Dae-dong, Gyeongsan, Kyoungbuk 712-749, South Korea
e-mail: tjko@yu.ac.kr

D. K. Baek
Institute of Mechanical Engineering Technology, Kyungpook National University, 1370, Sankyuk-dong, Puk-ku, Daegu 702-701, South Korea

1 Introduction

Semiconductor, electronics, aerospace, and automobile industries are all interested in advanced ceramics. Although the ceramics have superior mechanical properties, such as high hardness, wear resistance, high strength, and high-temperature stability, those properties are the reasons for the difficulty of machining. One promising solution for overcoming the machining difficulty is ultrasonic machining (USM) [1]. However, the cost of machining ceramic components by USM has been reported to be as high as 90 % of the total cost [2]. To this regard, various approaches to increase the material removal rate or reduce tool wear in case of titanium or its alloy were presented [3]. However, a more cost-effective method for machining ceramic components is needed [4].

Rotary ultrasonic machining (RUM) was developed as an alternative to USM. In RUM, axial vibration together with tool rotation does the machining, as shown in Fig. 1. Generally, RUM is considered a hybrid machining process that combines the material removal mechanisms of diamond grinding and USM [5]. Especially, its efficient removal of chips makes it a proper method for drilling microholes in brittle materials. The tool is a drill bit or endmill used in conventional drilling; however, an electroplated diamond abrasive grinding wheel or diamond-coated endmill could be used as an alternative [4, 5].

Since the introduction of RUM in 1964 [6, 7], extensive research has been carried out on its control variables (rotational speed, vibration amplitude and frequency, diamond type, size and concentration, bond type, coolant type, and pressure) and performance (material removal rate, cutting force, and surface roughness) [5, 8–14]. Some of the research focused on tool wear and edge chipping.

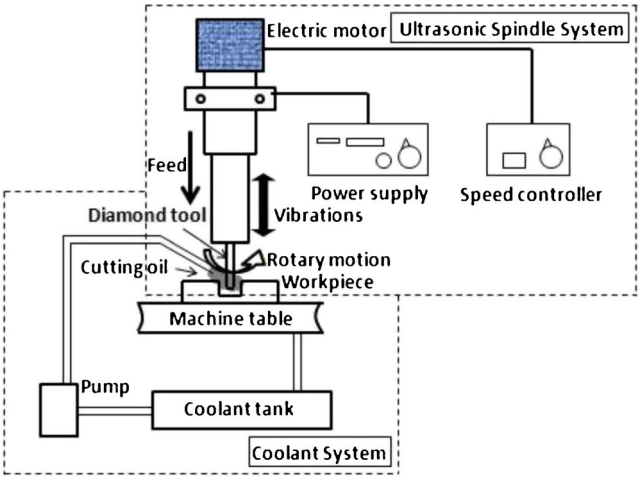

Fig. 1 System configuration of RUM

So far, in case of RUM, the tool has been core drill [4, 5] or cylindrical rod [15]. The coolant is circulated through the core of the drill; however, RUM does not need the slurry usually. Because of the tool shape or the inherent size of the core drill, the small hole drilling is not an easy matter even with RUM. In this paper, the sold type drill is used by considering the drilling of small hole on the ceramics without slurry. When drilling hard or brittle materials such as ceramics, in this paper, edge chipping at the exit of the hole is inevitable as shown in Fig. 2. In addition, the tool being so small wears abruptly. In order to solve the above problems, that is to reduce the edge chipping at the exit considering the tool wear, the cutting condition was optimized by response surface analysis and desirability functions to reduce both shortcomings. Experimental results showed the reduction in chipping that minimized tool wear while small hole drilling in ceramics.

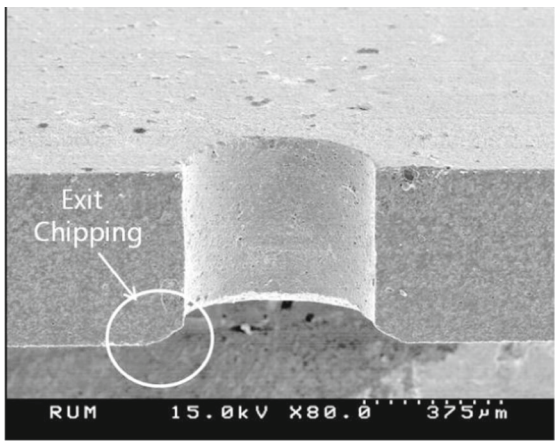

(Feed rate 13 μm/s, Ultrasonic power 25%, Spindle speed 2000 rpm)

Fig. 2 Scanning electron microscopy image of the cross-section of a microhole showing exit chipping (feed rate, 13 μm/s; ultrasonic power, 25 %; spindle speed, 2,000 rpm)

2 Experimental methods

2.1 Rotary ultrasonic machine and methods

A CNC milling machine (DMC Company, Korea) mounted with a rotary ultrasonic spindle system (G-NTS Company, Korea) was used in this experiment as shown in Fig. 3. The maximum ultrasonic power was 50 W, and the servo motor power was 700 W. The maximum spindle rotation speed, ultrasonic frequency, and amplitude were 3,000 rpm, 40 kHz, and 8 μm, respectively. The FANUC controller controlled these parameters as well as the depth feed rate. The cutting tool was the CVD diamond-coated drill (GCT GmbH, Germany) normally used in conventional drilling. Figure 4 shows the drill shape, which differs from the drill type normally employed such as the electroplated diamond-abrasive hollow cylindrical wheel. Coolant or lubricant was not supplied to the cutting area through the whole experiments. Alumina oxide ceramic of 96 % purity and thickness of 0.5 mm was used as its cutting material.

The workpiece, which was clamped on a special fixture using solid wax (Sonic-Mill wax #600-001, USA), was made from a high-molecular-weight glycol phthalate thermoplastic, which gradually polymerizes (becomes more brittle and hard) at its softening temperature of 74 °C. The degree of polymerization depends on the temperature at which it is used: the higher the temperature (up to a point), the more tenacious the bond (and difficulty of removal). Its properties start to degrade when the melted water-clear polymer starts to darken or

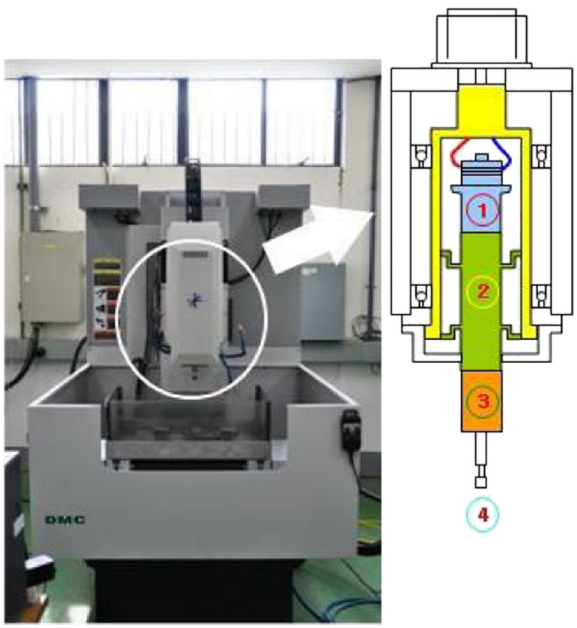

① Ultrasonic generator ② Horn ③ Tool holder ④ Tool

Fig. 3 Rotary Ultrasonic Machine and its internal structure with the ultrasonic spindle. *1* Ultrasonic generator, *2* horn, *3* tool holder, *4* tool

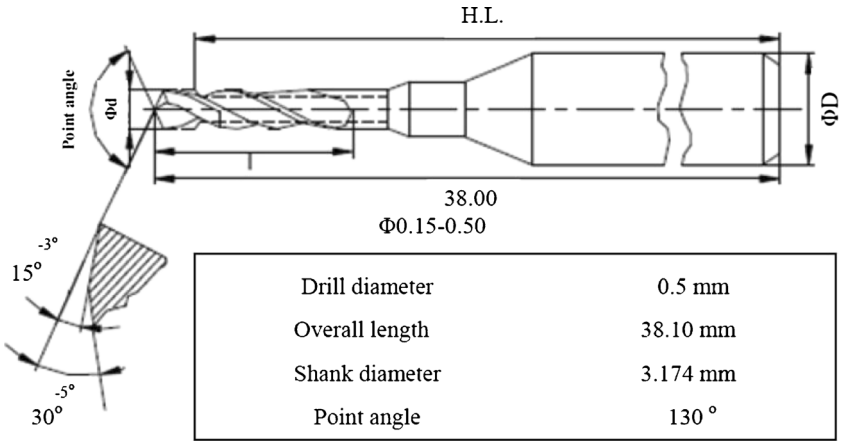

Drill diameter	0.5 mm
Overall length	38.10 mm
Shank diameter	3.174 mm
Point angle	130 °

Fig. 4 Drill shape used in the experiments

discolor. Generally, the medium should be used in the 75 to 80 °C range [16].

2.2 Design of experiments

Response surface experiments were carried out to identify the influence of each variable on tool wear and exit chipping to ultimately optimize these responses. Design factors, such as depth feed rate, spindle speed, and ultrasonic power, were chosen in advance based on the experiments. Ultrasonic power corresponds with the amplitude of tool axial vibration. Depth feed rate determines the penetration rate into the workpiece, and spindle speed is related to the rotational speed of the drill bit.

For the response surface analysis, a central composite design, representative of the response surface method, was chosen [17]. A cuboidal model, which determines the region of interest in central composite designs, was applied. The cuboidal model was used in a total of 17 (2^k+2k+n) experiments for three factors (k=3), which shows the factor cube point (2^k), axial point ($2k$), and center point (n=3, number of repeat experiments) [18]. Table 1 shows the levels of the independent variables necessary in the central composite method. Optical microscopy and scanning electron microscopy were used to measure the response or the machining results, such as exit chipping and tool wear.

Table 1 Level of factors

Level	Feed rate (μm/s)	Ultrasonic power (%) or tool amplitude (μm)	Spindle speed (rpm)
1.682	15	92 7.9	2,340
1	13	75 7.1	2,000
0	10	50 5.4	1,500
−1	7	25 2.5	1,000
−1.682	5	8 0.9	660

2.3 Experimental results

Exit chipping was measured for three experiments at the dominant crack position, as shown in Fig. 5. The values were then arithmetically averaged.

In addition, the tool wear in the flank face of the microdrill was measured for the same conditions of the chipping experiments and the values were averaged. Table 2 summarizes the values of the 17 experimental conditions.

3 Analysis of experimental results

3.1 Response surface analysis

The statistical analysis program MINITAB was used for the analysis of the response surface experiments. After constructing a response surface model using the experimental results from Table 3, a second-order polynomial regression model with respect to the responses was estimated by model adequacy. For the construction of the response surface model and estimation of the regression equation, a full quadratic model, which considers the shape of the response surface with respect to all design factors, was used. From the estimated second-order polynomial regression model, the adequacy of the underlying model was checked by residual analysis, adequacy of the analysis of variance (ANOVA), and the coefficient of determination.

3.2 Exit chipping

The adequacy of the response surface model of exit chipping due to RUM was mainly evaluated by residual analysis.

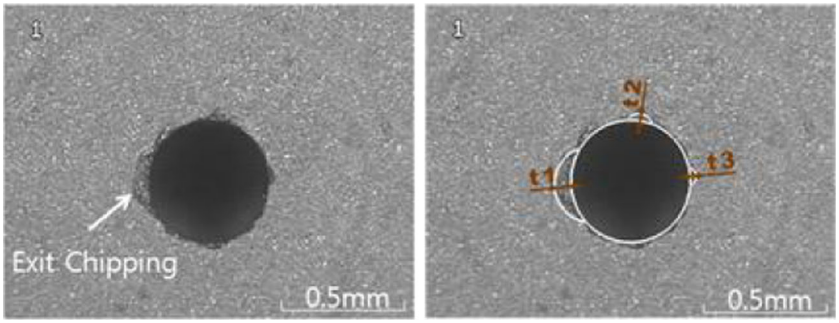

Fig. 5 Measurement of exit chipping (feed rate, 7 μm/s; ultrasonic power, 25 %; spindle speed, 1,000 rpm)

(Feed rate 7 μm /s, Ultrasonic power 25%, Spindle speed 1000 rpm)

Table 3 and Fig. 6 show the results of the ANOVA and residual analysis, respectively.

The coefficient of determination was 0.929, or the model had 92.9 % significance level. In addition, the probability of model inadequacy to the lack of fit was 0.009. Therefore, the model was considered adequate based on the reference significance level of 0.05.

From the results of the analysis, the second-order regression model was derived as a function of feed rate, ultrasonic power, and spindle speed as shown in Eq. (1):

$$Ec = 36.0414 - 9.7939f + 13.1206p - 25.0594r + 20.2768f^2 + 64.1876p^2 + 0.3526r^2 - 33.2535fp + 32.5535fr - 25.0453pr \quad (1)$$

where, Ec is exit chipping, f is feed rate, p is ultrasonic power, and r is rpm.

Table 2 Design of experiments and results

No.	Feed rate (μm/s)	Ultrasonic power (%)	Spindle speed (rpm)	Tool wear (μm)	Exit crack (μm)
1	7	25	1,000	17.214	67.00
2	13	25	1,000	18.704	59.67
3	7	75	1,000	24.217	137.00
4	13	75	1,000	36.225	56.33
5	7	25	2,000	18.232	40.33
6	13	25	2,000	17.039	53.67
7	7	75	2,000	21.720	49.00
8	13	75	2,000	42.169	40.67
9	5	50	1,500	18.232	60.00
10	15	50	1,500	26.751	62.00
11	10	8	1,500	15.709	91.67
12	10	92	1,500	31.348	118.00
13	10	50	660	24.096	61.00
14	10	50	2,340	26.569	21.00
15	10	50	1,500	19.315	36.67
16	10	50	1,500	20.517	34.00
17	10	50	1,500	20.482	35.67

3.3 Tool wear

Similarly, the response surface model for tool wear was estimated. Table 4 and Fig. 7 show the ANOVA results and the probability plot of the residual analysis, respectively. The coefficient of determination was 0.995. Alternatively, since the significance level was 95.5 %, the estimated model was deemed satisfactory. In addition, the probability of model inadequacy to the lack of fit was 0.06, so the model was considered adequate based on the reference significance level of 0.05.

As for the exit chipping, the estimation model for tool wear could be applied as a second-order regression model in Eq. (2).

$$Tw = 36.0414 - 9.7939f + 13.1206p - 25.0594r + 20.2768f^2 + 64.1876p^2 + 0.3526r^2 - 33.2535fp + 32.5535fr - 25.0453pr \quad (2)$$

where, Tw is the tool wear, f is feed rate, p is ultrasonic power, and r is rpm.

4 Process optimization

Based on estimated model, exit chipping and tool wear were optimized by using the desirability function.

Table 3 ANOVA table for exit chipping

Source	DF	Seq SS	Adj SS	Adj MS	F	P
Regression	9	13,583.9	13,583.9	1,509.32	10.22	0.003
Linear	3	4,336.3	4,336.3	1,445.42	9.79	0.007
Square	3	6,408.0	6,408.0	2,135.99	14.46	0.002
Interaction	3	2,839.7	2,839.7	946.56	6.41	0.020
Residual error	7	1,033.7	1,033.7	147.68		
Lack of fit	5	1,030.1	1,030.1	206.02	113.22	0.009
Pure error	2	3.6	3.6	1.82		
Total	16	14,617.6				

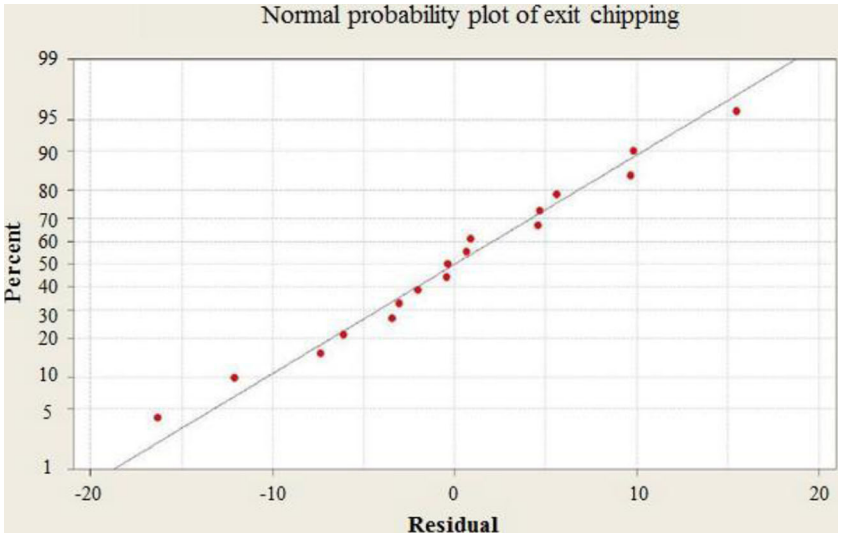

Fig. 6 Normal probability plot of the residuals for exit chipping

Table 4 ANOVA table for tool wear

Source	DF	Seq SS	Adj SS	Adj MS	*F*	*P*
Regression	9	813.729	813.729	90.414	16.54	0.001
Linear	3	628.388	628.388	209.463	38.31	0.000
Square	3	49.819	49.819	16.606	3.04	0.102
Interaction	3	135.523	135.523	45.174	8.26	0.011
Residual error	7	38.274	38.274	5.468		
Lack of fit	5	37.338	37.338	7.468	15.96	0.060
Pure error	2	0.936	0.936	0.468		
Total	16	852.004				

4.1 The desirability function

The desirability function is used for when multiple responses have to be combined into one response. Alternatively, it is the optimization of multiple responses when using the simultaneous optimization technique. Desirability is a measure of satisfaction of all the response objectives with respect to the solutions in the response optimization. Desirability is divided into individual (*d*) desirability and combined (*D*) desirability. Combined desirability ranges from 0 to 1, where 0 means one or more product characteristics are unacceptable, and 1 means that all product characteristics are on target.

Figure 8 shows the individual desirability function, whose minimum value indicates improvement. In other words, if the response value approaches the objective, desirability approaches 1, and if not, desirability comes to 0. In this research, a one-sided desirability function was chosen to minimize each response as follows [19].

$$d_i = \frac{Y_i - Y_{i\max}}{Y_{i\min} - Y_{i\max}} \tag{3}$$

where $Y_{i\min}$ and $Y_{i\max}$ are the minimum and the maximum values of response *i*, which are obtained from the mathematical

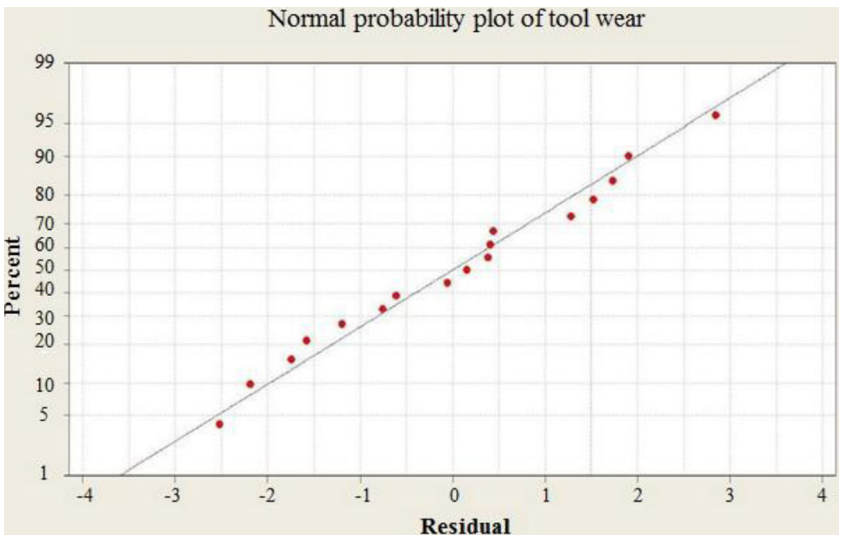

Fig. 7 Normal probability plot of the residuals for tool wear

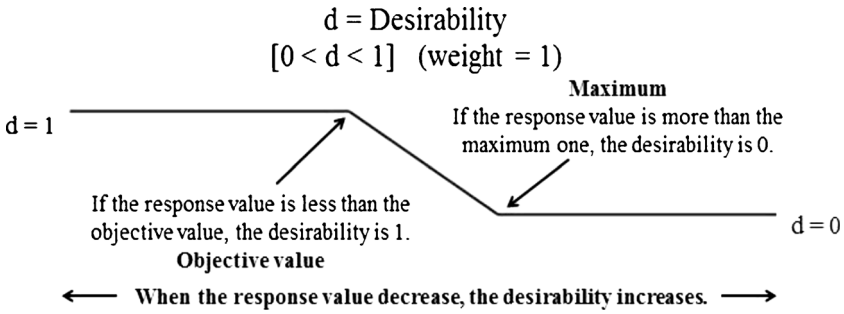

Fig. 8 Desirability function [19]

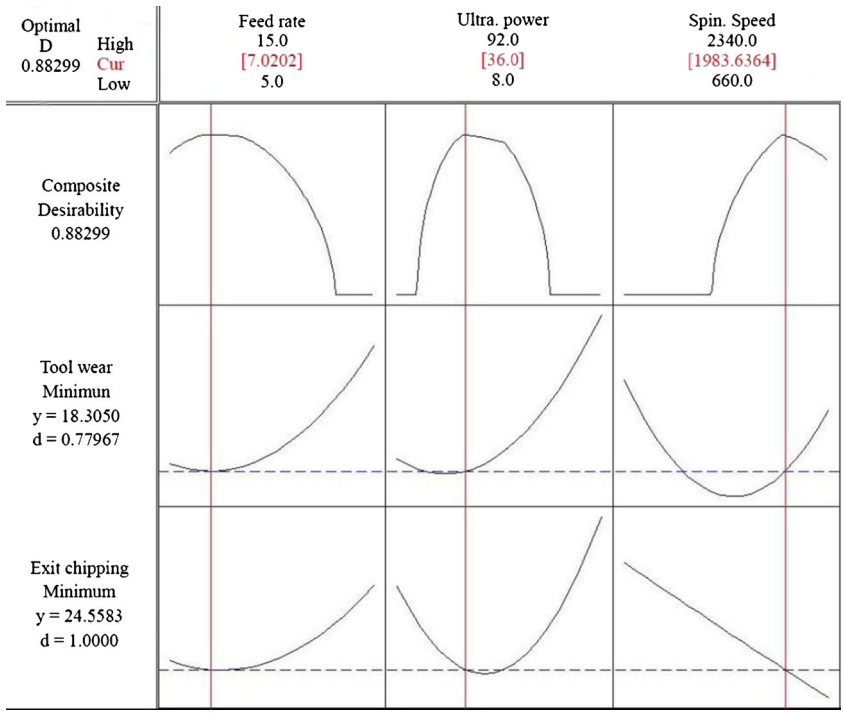

Fig. 9 Optimal cutting condition plot for RUM

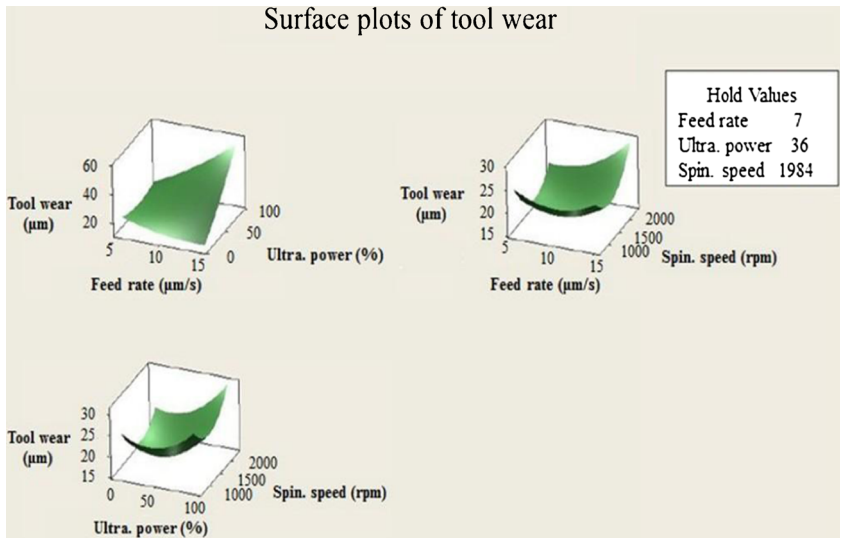

Fig. 10 Surface plot of tool wear

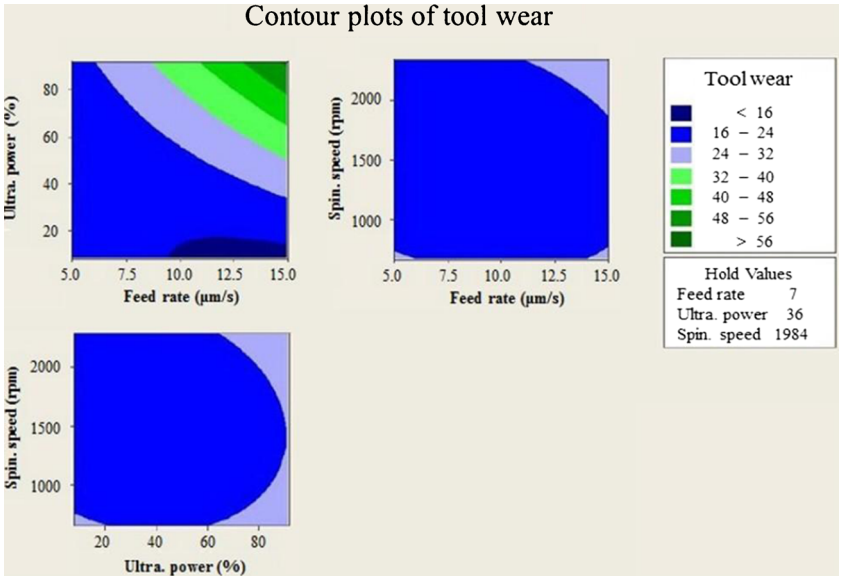

Fig. 11 Contour plot of tool wear

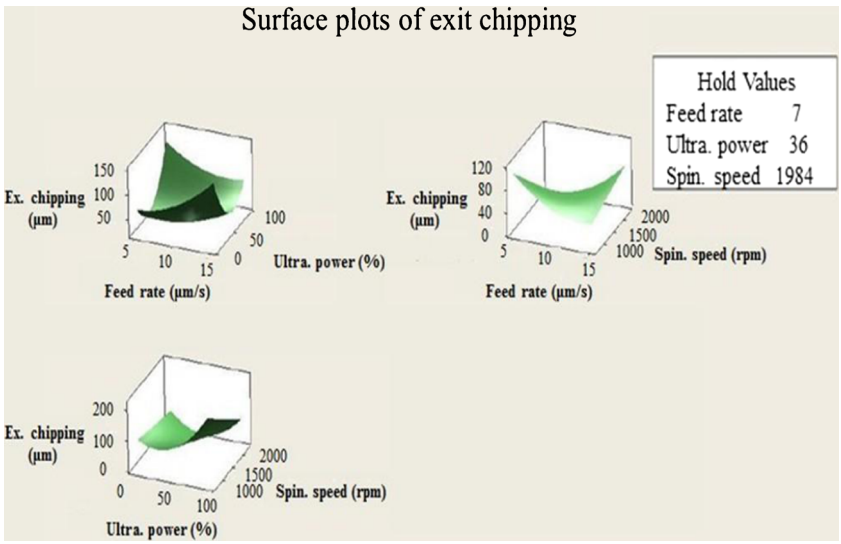

Fig. 12 Surface plot of exit chipping

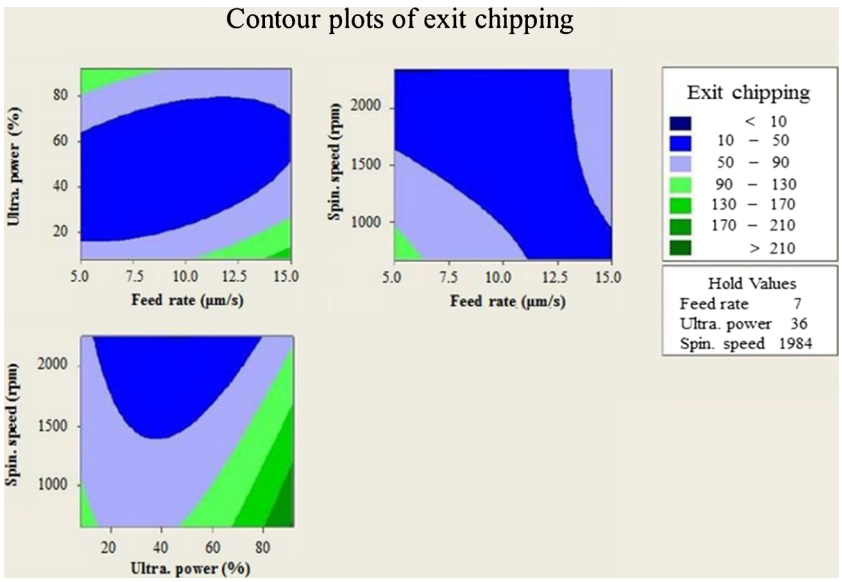

Fig. 13 Contour plot of exit chipping

Table 5 Multiple response analysis and experiment result under optimized process conditions

	Tool wear (μm)	Exit crack (μm)
Estimated response	18.305	24.558
Experiment results	16.891	25.378

model of Eqs. (1) and (2). Once these individual d_i functions are defined for all responses, they are combined into one objective function D, representing the overall desirability, which is calculated as the geometrical average of partial desirability functions [19].

$$D = \left[\prod_{i=1}^{m} d_i\right]^{1/m} \quad (4)$$

The overall desirability function D also varies from 0 to 1. If any d_i fails to meet the target requirements, the D will have a value of 0. On the other hand, if all responses are acceptable, the value of D will fall in the interval [0,1] and will increase with increasing individual desirability values.

4.2 Selection of optimal conditions

The desirability function was derived from the experimental data of exit chipping and tool wear. The weight of each response was set to 1 for the function. Figure 9 shows the optimal value of the response variable, as well as the level of each factor according to the level of change of the factor from the MINITAB. In the figure, D and d are the combined desirability and individual desirability for each characteristic value, respectively. The combined desirability is 0.88299 for feed rate of 7 μm/s, ultrasonic power of 36 %, and spindle speed of 1,984 rpm. From this result, the feed rate, that is the penetration rate of the tool into the workpiece, affects to chipping and tool wear. Also, the small axial amplitude of the vibration is necessary, and higher spindle speed is desirable that is related to the cutting speed as well as debris flushing.

4.3 Contour and surface plots

A contour plot expresses the response surface in a two-dimensional plane. The same response is presented on the same contour line. On the other hand, a surface plot expresses the response surface in three-dimensional space to explain the response values [17].

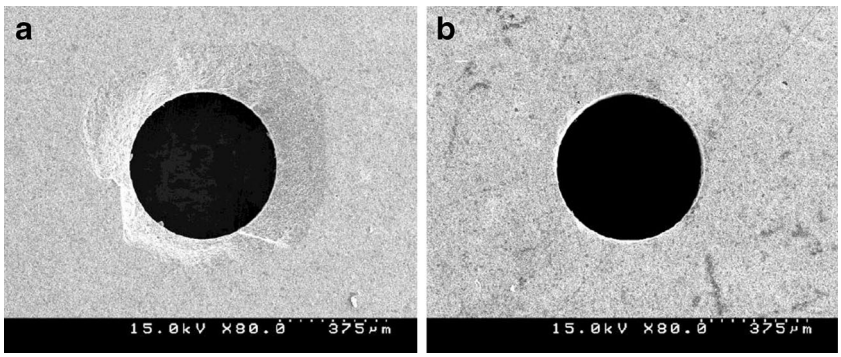

Fig. 14 Machining results at optimal cutting conditions: **a** without vibration (feed rate, 7.0 μm/s; ultrasonic power, 0 %; spindle speed, 1,984 rpm) and **b** after optimization with vibration (feed rate, 7.0 μm/s; ultrasonic power, 36.0 %; spindle speed, 1,984 rpm)

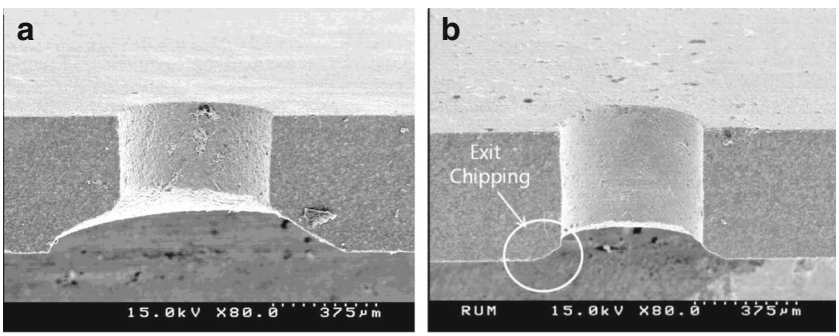

USM RUM

Fig. 15 Comparison with USM and RUM results: **a** ultrasonic machining (feed rate, 5 μm/s; ultrasonic power, 40 %; slurry ratio, 1:2), **b** rotary ultrasonic machining (feed rate, 7.0 μ m/s; ultrasonic power, 36.0 %; spindle speed, 1,984 rpm)

Figures 10, 11, 12, and 13 show the contour and surface plots according to the variation of each factor. After fixing the three conditions at the optimal values, the response surface was analyzed according the variation of the three factors that heavily influence the response. In the case of tool wear, from the response surface with respect to feed rate and spindle speed, we can see that tool wear can be reduced at the conditions along the higher values. Low ultrasonic power and high spindle speed decrease the amount of exit chipping.

To verify the regression model and the optimal conditions, a verification experiment was carried out with the optimal conditions. Table 5 shows the estimated response from the Eqs. (1) and (2) and its corresponding experimental results from the three experiments. The model could estimate the process well within the error range. Figure 14 shows the reduction of exit chipping based on the machining results. Compared with Fig. 2, Fig. 14 shows that RUM is more efficient for drilling microholes. Also, the comparison between USM and RUM is given in Fig. 15. As shown in the figure, the exit chipping was apparently reduced.

5 Conclusions

For microhole drilling on ceramic materials, even though USM is useful, RUM provides higher productivity and hole accuracy. In this research, exit chipping and severe tool wear, which are inevitable in hard material machining, were investigated. Response surface methodology was applied to analyze the influence of design factors, such as depth directional feed rate, ultrasonic power, and spindle speed on the reduction of exit chipping and tool wear. In addition, the desirability function was used for a multi-objective problem. Those tools gave the optimal conditions for reduced exit chipping and tool wear. From the optimization processes, low feed rate, adequate amount of axial vibration, as well as high cutting speed were selected as optimal parameters. From the experimental results, the tool wear and exit crack was decreased as 16.891 and 25.375 μm, respectively, which are declined several times more than the normal conditions. Therefore, this approach was verified effective for reducing exit chipping while restricting tool wear.

Acknowledgments The Basic Science Research Program through the National Research Foundation of Korea (NRF) funded by the Ministry of Education, Science and Technology (MEST) (Grant No. 2011-0013496) supported this work.

References

1. Singh R, Khamba JS (2006) Ultrasonic machining of titanium and its alloys: a review. J Mater Process Technol 173:125–135
2. Jahanmir S, Ives LK, Ruff AW, Peterson MB (1992) Ceramic machining: assessment of current practice and research needs in the United States, NIST Special Publication 834
3. Singh R, Khamba JS (2007) Macromodel for ultrasonic machining of titanium and its alloys: designed experiments. J Eng Manuf 221(2): 221–229, 9
4. Li ZC, Cai L, Pei ZJ, Treadwell C (2006) Edge-chipping reduction in rotary ultrasonic machining of ceramics: finite element analysis and experimental verification. Int J Mach Tools Manuf 46:1469–1477
5. Zeng WM, Li ZC, Pei ZJ, Treadwell C (2005) Experimental observation of tool wear in rotary ultrasonic machining of advanced ceramics. Int J Mach Tools Manuf 45:1468–1473
6. Legge P (1964) Ultrasonic drilling of ceramics. Ind Diam Rev 24(278):20–24
7. Legge P (1966) Machining without abrasive slurry. Ultrasonic 4(3): 157–162
8. Pei ZJ, Ferreira PM (1998) Modeling of ductile-mode material removal in rotary ultrasonic machining. Int J Mach Tools Manuf 38: 1399–1418
9. Li ZC, Jiao Y, Deines TW, Pei ZJ, Treadwell C (2005) Rotary ultrasonic machining of ceramic matrix composites: feasibility study and designed experiments. Int J Mach Tools Manuf 45: 1402–1411
10. Liu J, Zhang D, Qin L, Yan L (2012) Feasibility study of the rotary ultrasonic elliptical machining of carbon fiber reinforced plastics (CFRP). Int J Mach Tools Manuf 53:141–150
11. Liu D, Cong WL, Pei ZJ, Tang Y (2012) A cutting force model for rotary ultrasonic machining of brittle materials. Int J Mach Tools Manuf 52:77–84
12. Hu P, Zhang JM, Pei ZJ, Treadwell C (2002) Modeling of material removal rate in rotary ultrasonic machining: designed experiments. J Mater Process Technol 129:339–344
13. Ya G, Qin HW, Yang SC, Xu YW (2002) Analysis of the rotary ultrasonic machining. J Mater Process Technol 129: 182–185
14. Gong H, Fang FZ, Hu XT (2010) Kinematic view of tool life in rotary ultrasonic side milling of hard and brittle materials. Int J Mach Tools Manuf 50:303–307
15. Wiercigroch M, Neilson RD, Player MA (1999) Material removal rate prediction for ultrasonic drilling of hard materials using an impact oscillator approach. Phys Lett A 259(2):91–96
16. www.sonicmill.com (2012) Sonicmill Company
17. Chun SH, Ko TJ (2011) Study on the response surface model of machining error in internal lathe boring. Int J Precis Eng Manuf 12: 177–182
18. Montgomery DC (2005) Design and analysis of experiments. Wiley, New York, pp 405–463
19. Fuller D, Scherer W (1998) The desirability function: underlying assumptions and application implications. University of Charlottesville, VA, 22903